DOI: 10.1002/cbic.200500116

Adsorption of Amyloid β (1–40) Peptide at Phospholipid Monolayers

Elena Maltseva,[a] Andreas Kerth,[b] Alfred Blume,[b] Helmuth Möhwald,[a] and Gerald Brezesinski*[a]

The folding of amyloid β (1–40) peptide into β-sheet-containing fibrils is thought to play a causative role in Alzheimer's disease. Because of its amphiphilic character, the peptide can interact with phospholipid membranes. Langmuir monolayers of negatively charged DPPS, DPPG, and DMPG, and also of zwitterionic DPPC and DMPC, have been used to study the influence of the peptide on the lipid packing and, vice versa, the influence of phospholipid monolayers on the peptide secondary structure by infrared reflection absorption spectroscopy and grazing incidence X-ray diffraction. The peptide adsorbs at the air/water (buffer) interface, and also inserts into uncompressed phospholipid monolayers. When adsorbed at the interface, the peptide adopts a β-sheet conformation, with the long axis of these β-sheets oriented almost parallel to the surface. If the lipid exhibits a condensed monolayer phase, then compression of the complex monolayer with the inserted peptide leads to the squeezing out of the peptide at higher surface pressures (above 30 mN m^{-1}). The peptide desorbs completely from zwitterionic monolayers and negatively charged DPPG and DPPS monolayers on buffer, but remains adsorbed in the β-sheet conformation at negatively charged monolayers on water. This can be explained in terms of electrostatic interactions with the lipid head groups. It also remains adsorbed at, or penetrating into, disordered anionic monolayers on buffer. Additionally, the peptide does not influence the condensed monolayer structure at physiological pH and modest ionic strength.

Introduction

Some neurodegenerative diseases, such as Alzheimer's disease, Down's syndrome, and hereditary cerebral hemorrhagic disease, are characterized by the presence of amyloid plaque in the brain. The major components of this plaque are small peptides of 39–43 amino acids—amyloid β (Aβ) peptides. The most common are the peptides with 40 and with 42 amino acids. The more hydrophobic 42-residue peptide is thought to play a seed role in plaque formation, but the 40-amino acid peptide can also precipitate in the absence of longer peptides. Aβ peptides are the products of proteolytical cleavage of a membrane-anchored protein—amyloid precursor protein (APP).[1] The peptides are amphipathic; they include the transmembrane and extracellular parts of APP. Normally they are present in cerebrovascular fluids and blood in a soluble form.[2] During aging or as a result of disease they precipitate into amyloid fibrils in a process thought to include a conformation change of soluble Aβ (in either random coil or α-helical conformation) into β-sheet strands.[3–6] The fibrils have been shown to be neurotoxic,[7] but the mechanisms of their toxicity and of their formation are still unclear. Many factors influence these processes: overexpression of Aβ(1–42) can accelerate fibril formation,[8] a change in the membrane composition can induce conformation changes in Aβ, or, vice versa, the peptide can influence membrane properties such as fluidity, permeability, and curvature.[9–14] It has also been reported that Aβ takes part in neuroinflammation and oxidation processes.[15]

This work focuses on interactions of membrane phospholipids with Aβ (1–40) and their implications for peptide folding. Most researchers agree that neutral membranes have no effect on the peptide, whereas negatively charged membranes induce the conformational change of Aβ from random coil to α-helix or to β-sheet with further aggregation.[16,17] The presence of ions,[18] the ratio between lipid and peptide,[16,17] and the presence of cholesterol and gangliosides[10,19,20] all influence the change in the peptide secondary structure.

Since biological membranes can be viewed as two weakly coupled monolayers, Langmuir monolayers represent a convenient model system with which to mimic their surfaces. Development of such precise techniques as Grazing Incidence X-ray Diffraction (GIXD) and Infrared Reflection Absorption Spectroscopy (IRRAS) allows the characterization of structures formed by phospholipid molecules at air/water interfaces,[21,22] as well as the secondary structures and orientations of adsorbed peptides,[23–25] and so we have used a combination of these techniques to determine the possible interactions between phospholipids and Aβ peptide. This study has made use of zwitterionic and anionic phospholipids exhibiting different

[a] *E. Maltseva, Prof. Dr. H. Möhwald, Dr. G. Brezesinski*
Max Planck Institute of Colloids and Interfaces
Am Mühlenberg 1, 14476 Golm/Potsdam (Germany)
Fax: (+49) 331-567-9202
E-mail: gerald.brezesinski@mpikg.mpg.de

[b] *Dr. A. Kerth, Prof. Dr. A. Blume*
Institute of Physical Chemistry
Martin Luther University Halle–Wittenberg
Mühlpforte 1, 06099 Halle/Saale (Germany)

phase behavior: 1,2-dipalmitoylphosphatidylcholine (DPPC), 1,2-dimyristoylphosphatidylcholine (DMPC), 1,2-dipalmitoylphosphatidylglycerol (DPPG), 1,2-dimyristoylphosphatidylglycerol (DMPG), and 1,2-dipalmitoylphosphatidylserine (DPPS).

Results

Aβ peptide displays pronounced surface activity, adsorbing at air/water (or buffer) interfaces as well as at uncompressed phospholipid monolayers at zero pressure.[26] During adsorption to a pure air/water interface or to uncompressed zwitterionic monolayers, the surface pressure increases to approximately 18 mN m^{-1}. However, adsorption of Aβ at uncompressed negatively charged monolayers on water results in higher values for the equilibrium surface pressure (above 20 mN m^{-1}.). Ege and Lee[27] have shown that Aβ is not able to insert into compressed zwitterionic monolayers if the lateral pressure is above 25 mN m^{-1}, but it does insert into negatively charged monolayers even at surface pressures of 30 mN m^{-1}.

IRRAS was applied to detect the presence of Aβ and its secondary structure at the interface. During Aβ adsorption at the air/water interface or insertion into uncompressed phospholipid monolayers, amide bands in the region between 1700–1500 cm^{-1} (amide I: 1700–1620 cm^{-1} and amide II: 1580–1520 cm^{-1}) appear and grow (Figure 1). After 3–4 h of adsorption, no further increase of the amide band intensities was observed.

In order to compare spectra of Aβ adsorbed at the air/water (buffer) interface and on lipid monolayers, the pure lipid spectra were subtracted from mixed lipid/peptide spectra. The remaining peptide spectra are very similar to the spectra of the pure peptide adsorbed at an air/water (buffer) interface. The positions of the amide bands do not depend on the type of lipid (zwitterionic or negatively charged). The most intense band in the amide I region was observed at 1627 cm^{-1} with a shoulder at 1690 cm^{-1}, indicating an antiparallel β-sheet conformation of the peptide at the interface (Figure 2). The shoulder of the amide I band in the 1648–1658 cm^{-1} region reveals the presence of a small amount of random coil or α-helical conformation, whilst the shoulder at 1674 cm^{-1} may be attributable to a β-turn or to residual trifluoroacetic acid (TFA).[25] Amide II bands are rarely used for secondary structure determination, but two major contributions were found in the amide II region of the Aβ spectra. The most intense contribution, at around 1530 cm^{-1}, indicates the presence of a β-sheet structure, while a band at around 1550 cm^{-1} can be attributed to random coil, α-helix, or β-turn conformation.[28,29] Aβ peptide adsorbed at the interface thus exists mainly in a β-sheet conformation, although our CD spectroscopy experiments clearly show that it has predominantly random coil conformation when dissolved in water and buffer at pH 7.5 after the pretreatment described in the Experimental Section. No change in the IRRA band positions was observed during the adsorption process. The peptide spectra are similar to those obtained for aggregated Aβ. Either only the small part of the peptide already existing in β-sheet conformation in the bulk adsorbs at the interface or the conformational transition from mainly random coil to mainly β-sheet at the interface is too fast to be detected.

IRRAS was also employed to determine the orientation of the peptide at the interface. For this purpose, spectra were acquired with *p*-polarized light at various angles of incidence (Figure 3). The *p*-polarized light probes the dipole moment components parallel and perpendicular to the surface, and molecular orientations can consequently be determined. In contrast, *s*-polarized light probes only the dipole moment component parallel to the surface, so the corresponding negative reflectance–absorbance values increase monotonically with increasing incidence angle and do not allow detailed information about the anisotropy of the film to be obtained.

The amide I band (1627 cm^{-1} and 1690 cm^{-1}) is associated with the peptide C=O stretching vibration and in the case of β-sheets it splits into two components.[30] The transition dipole moment of the more intense contribution at 1627 cm^{-1} is oriented along the plane of the interchain hydrogen bonds, perpendicular to the peptide chain, and the less intense contribu-

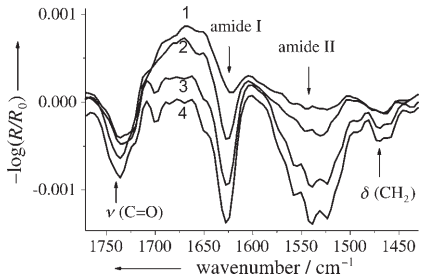

Figure 1. IRRA spectra of Aβ adsorbing at a DPPC monolayer (p_0 = 0 mN m^{-1}, A_0 = 96 Å^2 molecule^{-1}) on water taken at different times: 1) 5 min, 2) 50 min, 3) 120 min, 4) 180 min. The peptide concentration was 0.185 μM and the final surface pressure was 15 mN m^{-1}. All spectra were recorded at an angle of incidence of 40° with use of *s*-polarized light.

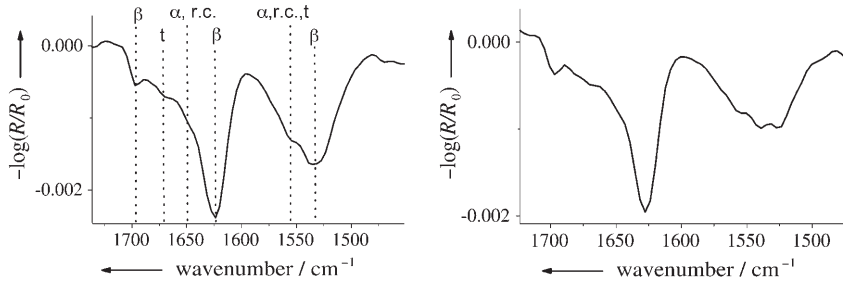

Figure 2. IRRA spectra of Aβ adsorbed at a pure air/buffer interface (p = 14 mN m^{-1}, left) and at a DPPG monolayer (16 mN m^{-1}, right). The adsorption process started at an initial area per lipid of 96 Å^2. The corresponding spectrum of a pure DPPG monolayer recorded at the same area per molecule was subtracted. All spectra were recorded at an angle of incidence of 40° with use of *s*-polarized light. The letters β (β-sheet), t (turn), α (α-helix), and r.c. (random coil) indicate the positions of the corresponding bands.

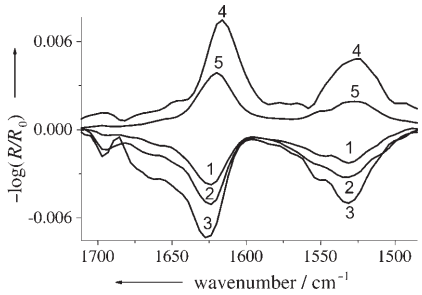

Figure 3. IRRA spectra of Aβ (0.185 μM) adsorbed at the air/buffer interface acquired with *p*-polarized light at various incident angles: 1) 32°, 2) 40°, 3) 48°, 4) 56°, 5) 62°. The surface pressure was 15 mN m^{-1}.

tion at 1690 cm^{-1} is oriented along the peptide chain. The amide II band results from C–N stretching and N–H bending vibrations, and its transition dipole moment is oriented along the peptide chain. The presence of a layer (e.g., lipid monolayer, adsorbed peptide) at the air/water interface results in the appearance of the O–H stretching band at 3800–3000 cm^{-1} and the H_2O bending band in the region of the amide bands (1700–1600 cm^{-1}), which produces additional difficulties in the determination of the peptide secondary structure. The intensities of these bands depend on the layer thickness and refractive index.[31,32] Simulations of amide bands for a β-sheet oriented parallel to the interface with different angles of incidence and use of *p*-polarized light are shown in Figure 4. A

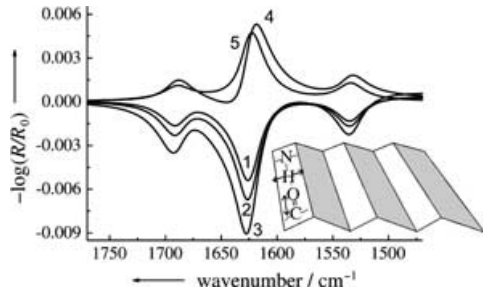

Figure 4. Simulation of IRRA spectra of a β-sheet lying flat at the air/water interface. The calculation was performed for *p*-polarized light and different angles of incidence—1) 32°, 2) 40°, 3) 48°, 4) 56°, 5) 62°—for the amide I bands at 1627 and 1690 cm^{-1} and the amide II band at 1535 cm^{-1}.

film thickness of 10 Å and the corresponding extinction coefficients for a model antiparallel β-sheet were used for the calculation.[33] The simulation assumes a uniaxial distribution of the β-sheet relative to the surface normal, or at least a uniaxial distribution of peptide domains. This assumption is supported by the GIXD results, as the peptide shows a 2D powder diffraction pattern (Figure 8, below). The calculated IRRA spectra include the simulation of the H_2O bending mode of the subphase at about 1645 cm^{-1}, as the refractive index and the absorption coefficient of H_2O are parts of the simulation.[34] The influence of the calculated H_2O baseline is not very pronounced, but it is responsible for the slightly asymmetric band shape at higher frequencies of the amide I band.[23] The asymmetric band shape in the experimentally measured spectra might additionally arise from other secondary structure elements such as α-helix, random coil, or β-turn (Figure 2). The use of D_2O as subphase was avoided, both because of the easier use of H_2O and because increasing amounts of HOD in the subphase during long-term measurements, such as adsorption measurements, sometimes caused baseline problems. A spectral simulation with D_2O would be easier as there are no solvent-related vibrations in the amide I region.

Comparison of measured and simulated spectra reveals that Aβ is lying almost flat at the air/water interface, although a slightly tilted conformation cannot be excluded. The orientation of the peptide penetrated into a phospholipid monolayer is the same as at the pure air/water interface (spectra not shown). This indicates that the presence of an uncompressed phospholipid monolayer does not affect either the secondary structure or the orientation of the peptide.

Additionally, IRRAS provides information about the state of the lipid aliphatic chains in a monolayer.[34] The symmetrical (2849–2855 cm^{-1}) and asymmetrical (2916–2925 cm^{-1}) stretching modes of CH_2 groups are sensitive to conformational order and packing of the hydrocarbon chains.[35,36] In the liquid-expanded state, the appearance of *gauche* conformations shifts the CH_2 modes to approximately 2924 cm^{-1} and 2855 cm^{-1}. In a condensed state, these bands are located at smaller values (approximately 2919 cm^{-1} and 2850 cm^{-1}), indicating that the aliphatic chains are in all-*trans* conformation.

The lipids used in this work show different phase behavior at room temperature. DPPC exhibits a phase transition from liquid-expanded (LE) to a condensed (LC) state during compression both on buffer and on water, DPPS is fully condensed on water and buffer, whilst DPPG on water is condensed, but on buffer it exhibits a LE/LC transition at approximately 10 mN m^{-1}. Such a difference in the phase behavior can be explained by different ionization states of DPPG on buffer and on water:[37–39] only 10–20% of DPPG molecules are ionized on water, whereas DPPG is fully ionized on buffer at pH 7.5.

It had previously been found that the phase behavior of zwitterionic 1,2-dimyristoylphosphatidylethanolamine (DMPE) and 1,2-dipalmitoylphosphatidylethanolamine (DPPE) is not influenced by Aβ adsorption.[26] The same is also observed for DPPC both on water and on buffer. At zero pressure, the peptide penetrates into the surface area not occupied by lipids and compresses them; this induces the phase transition in DPPC and DMPE monolayers. Since the transition pressure is the same on water and on the peptide solution, one can conclude that the peptide does not specifically interact with the zwitterionic lipids. Similar results were obtained for DPPG on buffer (pH 7.5). Therefore, it is unlikely that the peptide specifically interacts with these phospholipids at physiological pH values. The phase state of the lipid chains is also not influenced by the peptide, although a small shift in the CH_2 stretching modes of anionic lipids on water indicates a slight perturbation of the chain ordering.

Compression of lipid monolayers with inserted Aβ results in the squeezing out of the peptide at lateral pressures above

30 mN m^{-1}. At high surface pressures (40–45 mN m^{-1}) the monolayer occupies the same area per lipid molecule as the pure lipid monolayer on water or buffer. Expansion results in a reinsertion of the peptide into the monolayer at surface pressures below the equilibrium value of 16–18 mN m^{-1}. IRRAS measurements show that the amide bands disappear completely from the IRRA spectra of zwitterionic monolayers on water and buffer, as well as those of anionic monolayers on buffer, at surface pressures above 30 mN m^{-1}. This establishes that the peptide might even be desorbed from these monolayers. A different situation was observed for anionic monolayers on water, with the amide I band intensity decreasing and shifting to slightly larger wavenumbers (from 1627 to 1630 cm^{-1}), but the bands do not disappear completely.

To check the specific adsorption of the peptide at compressed monolayers, another procedure was applied. Before peptide injection, the monolayers were compressed to 30 mN m^{-1}. After injection, the peptide did not adsorb at compressed zwitterionic monolayers on both water and buffer. In this case, the monolayer spectra are identical to pure phospholipid spectra, no amide bands appear even after 24 h of adsorption. In the case of negatively charged monolayers on water, Aβ injection results in the appearance of amide bands (Figure 5) and increases in the intensities of the water bands

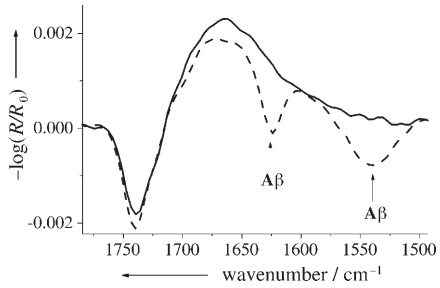

Figure 5. IRRA spectra of a DPPG monolayer on buffer (solid line) and on water (dashed line). Spectra were taken one day after Aβ (40 μg, 0.92 μM) injection, the surface pressure being kept constant at 30 mN m^{-1}. All spectra have been recorded at an angle of incidence of 40° with use of *s*-polarized light.

(Figure 6). The latter factor indicates an increasing surface layer thickness due to Aβ adsorption. The most intense band in the amide I region is observed at 1630 cm^{-1}; this position can again be attributed to β-sheet conformation. The reason for the shift of the amide I band to larger wavenumbers could be a reduction in the crystallinity of the adsorbed β-sheet induced by a more hydrophilic environment in the vicinity of the phospholipid head groups, an assumption supported by the disappearance of the Bragg peak arising from the β-sheet structure in GIXD experiments (see below). On buffer, however, no peptide adsorption was observed (Figure 5). Furthermore, injection of NaCl into the subphase beneath a DPPG monolayer compressed to 30 mN m^{-1} with adsorbed Aβ results in the disappearance of the peptide signal (Figure 6). This can be explained by competitive adsorption of counterions. It is interesting to note that the presence of adsorbed peptide slightly increases the intensity of the phosphate band centered at around 1222 cm^{-1}; this indicates a higher degree of ionization of DPPG on the peptide subphase than on pure water. Additionally, the band position shows that the phosphate group is slightly dehydrated in the presence of Aβ. On the salt solution, the phosphate band shifts to 1217 cm^{-1} and becomes even more intensive. This observation reveals a higher degree of ionization of the now better hydrated DPPG phosphate group in the presence of NaCl.[40]

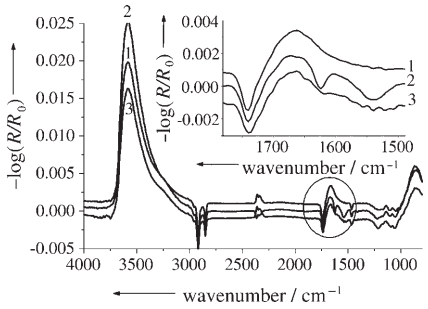

Figure 6. IRRA spectra of a DPPG monolayer (amide region) on water (curve 1), three hours after injection of Aβ (40 μg; curve 2), and one day after addition of salt (curve 3). The final Aβ concentration was 0.92 μM, and the final salt concentration was 50 mM. The IRRA spectrum of DPPG has been shifted to 0.001 and that of DPPG on Aβ + salt to −0.001 for clarity. The surface pressure was kept constant at 30 mN m^{-1}.

The structures of the DPPG and DPPC monolayers were investigated by GIXD experiments. The monolayers were compressed to a desired pressure, which was kept constant automatically, and diffraction data were taken. Selected contour plots of the corrected X-ray intensities as a function of the in-plane (Q_{xy}) and out-of-plane (Q_z) components of the scattering vector for DPPG monolayers on different subphases are shown in Figure 7. At low surface pressure, three diffraction peaks can be detected for DPPG on water. Such a peak distribution indicates the existence of an oblique chain lattice with molecules

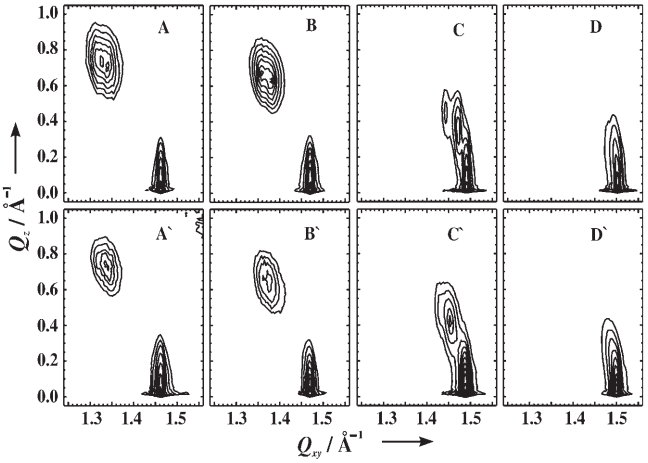

Figure 7. Contour plots of the corrected X-ray intensities as a function of the in-plane component (Q_{xy}) and the out-of-plane component (Q_z) of the scattering vector for DPPG on buffer at pH 7.5: A) 20 mN m^{-1}, B) 30 mN m^{-1}, DPPG on Aβ (0.3 μM) in buffer at pH 7.5: A′) 20 mN m^{-1}, B′) 30 mN m^{-1}, DPPG on water C) 20 mN m^{-1}, D) 30 mN m^{-1}, and DPPG on Aβ (0.3 μM) in water C′) 22 mN m^{-1}, D′) 30 mN m^{-1}.

tilted in a direction intermediate between nearest (NN) and next-nearest (NNN) neighbor direction. Increasing pressure results in a shift to larger Q_{xy} and smaller Q_z values. This can be easily understood, because increasing lateral pressure decreases the tilt angle of the aliphatic chains. The phase transition to hexagonal packing of upright oriented molecules takes place between 30 mN m^{-1} and 40 mN m^{-1}. The peak positions obtained on buffer differ from those obtained on water, being shifted to lower Q_{xy} and higher Q_z values indicating larger unit cell areas and larger tilt angles of the aliphatic chains. Transition to hexagonal packing cannot be achieved even at very high surface pressures. At 40 mN m^{-1}, the tilt angle still amounts to 26°. Obviously, the increased degree of ionization of the DPPG head group at higher pH and salt concentrations results in increased repulsion between molecules and in the reorientation of the head groups. The mismatch between the head group size and the size of the two aliphatic chains results in the tilted structure being observed at all pressures. DPPC on water exhibits behavior similar to that of DPPG on buffer, due to the large phosphatidylcholine head group. The lattice parameters and tilt of the chains do not change at different ion concentrations and over a large pH range, since DPPC is a zwitterionic lipid.[41] The large width of the diffraction peaks (due to small correlation length) is the reason for greater uncertainty in the determination of the molecular tilt.

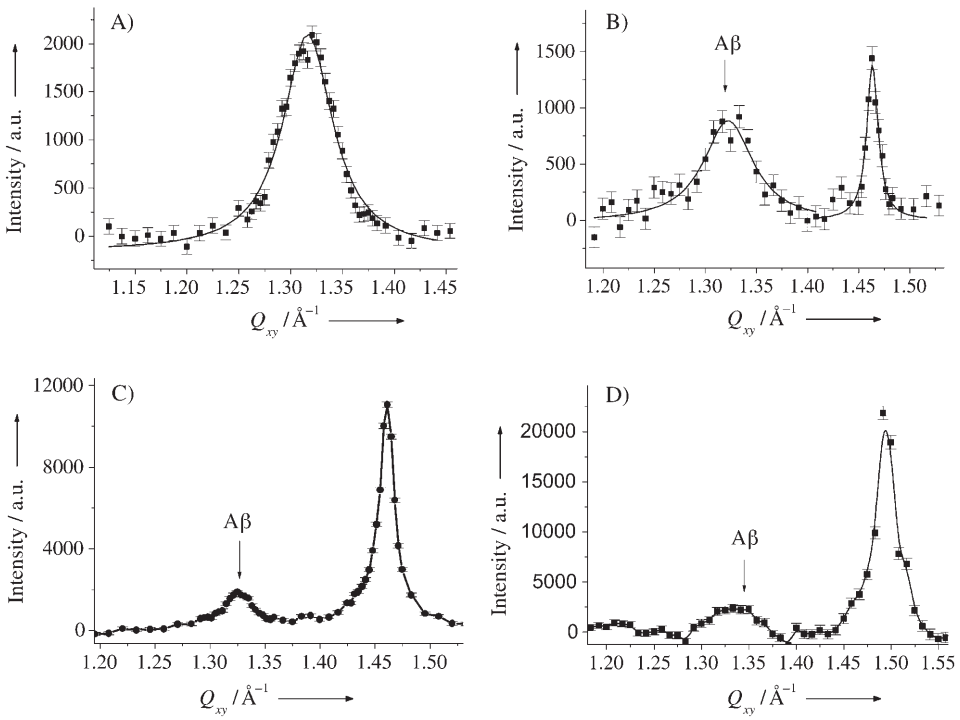

Figure 8. Integrated intensity over a Q_z range between −0.05 and 0.3 Å^{-1} as a function of Q_{xy} for Aβ adsorbed at the air/water interface at 14 mN m^{-1} (A), adsorbed at a DPPC monolayer on water at 10 mN m^{-1} (B), adsorbed at a DPPG monolayer on buffer at 18 mN m^{-1} (C), and adsorbed at a DPPG monolayer on water at 20 mN m^{-1} (D). The peak at 1.33 Å^{-1} originates from the β-sheet structure of Aβ, whilst that between 1.45 and 1.5 Å^{-1} corresponds to the lipid monolayer.

The GIXD measurements were performed on Aβ solution (0.3 μM), starting from the equilibrium pressure reached after 3 h of Aβ adsorption. Comparison of the diffraction peak positions shows that the chain lattices of DPPC on water and DPPG on buffer are not changed by insertion of the peptide. The slightly higher tilt of DPPG on Aβ in water can be explained in terms of electrostatic interactions with the peptide, which result in an increased ionization state of the lipid.

The peptide adsorbed at the air/water interface or at lipid monolayers at low surface pressure shows a weak Bragg peak at $Q_{xy} = 1.33$ Å^{-1} ($\Delta Q_{xy} = 0.065$ Å^{-1}) and zero Q_z (Figure 8). This peak corresponds to a repeat distance of 4.7 Å, which is the spacing between hydrogen-bonded peptide chains in a β-sheet structure. In some cases, an additional Bragg peak with a d-spacing of 39.3 Å was found. The origin of this peak is still unclear.[42] The weak peak at 1.33 Å^{-1} was not observed in the diffraction patterns taken at surface pressures above 30 mN m^{-1}. The strong peak between 1.45 and 1.5 Å^{-1} (Figure 8B–D) arises from the phospholipid chain lattice.

Aβ adsorbs at compressed (30 mN m^{-1}) anionic monolayers on water but not on buffer. The adsorption is unspecific and can be ascribed to enhanced electrostatic interactions at low ionic strength. The question that now arises is whether the lipid phase state is important for the adsorption process. POPG, DMPG, and DMPC monolayers, which exist in the liquid expanded (LE) state under the experimental conditions, are used for comparison. The same behavior as described for condensed monolayers was observed at 30 mN m^{-1}, but an interesting difference between condensed (LC) and disordered (LE) monolayers could be seen when the peptide was first inserted into the monolayer on buffer at low pressure. In the case of the condensed monolayers, the compression resulted in a complete squeeze-out of the peptide at higher surface pressures. In contrast, Aβ remained in the anionic monolayer upon compression to 30 mN m^{-1}. The transition from LE to LC occurs for DMPG between 37 and 41 mN m^{-1}. The peptide is squeezed out and desorbed (disappearance of IRRAS signal) only when the condensed phase is formed (Figure 9). The peptide also remains adsorbed at or penetrated into the DMPG monolayer on water at 30 mN m^{-1} after addition of salt. Obviously, only the combination of electrostatic and hydrophobic interactions stabilizes the peptide in disordered anionic monolayers, because it leaves the disordered zwitterionic DMPC monolayer at high surface pressure.

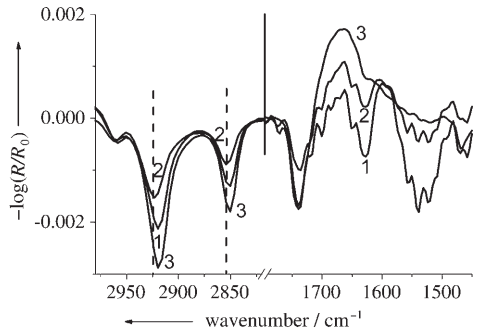

Figure 9. IRRA spectra in the CH_2 stretching and amide regions of DMPG monolayers in the presence of Aβ (40 μg, 0.92 μM): 1) on water at 30 mN m^{-1}, 2) on water + NaCl at 30 mN m^{-1}, and 3) on water + NaCl at 50 mN m^{-1}. At 30 mN m^{-1} the DMPG monolayer on water exists in a condensed phase, whilst on buffer it is in the LE phase. The phase transition from LE to LC occurs on buffer at around 40 mN m^{-1}. The spectra were acquired with use of *s*-polarized light and at an angle of incidence of 40°.

Discussion

The secondary structure of Aβ adsorbed at a pure air/water (buffer) interface or at phospholipid monolayers has been determined by the IRRAS experiments. The data clearly demonstrate that the peptide adopts a β-sheet conformation at the interface, the β-sheets being oriented parallel to the interface. The result is supported by GIXD investigations, which reveal a Bragg peak arising from the adsorbed peptide β-sheets with a characteristic repeat distance of 4.7 Å. Both the air/water interface and phospholipid monolayers in an uncompressed state can be viewed as hydrophobic/hydrophilic interfaces, therefore we assume that Aβ is attracted by such hydrophobic interfaces and that increasing surface concentration of Aβ is responsible for the observed conformational change in the secondary structure from random coil to β-sheet. A similar result was previously observed by Kowalewski and Holtzman,[43] who found that Aβ forms uniform elongated sheets on hydrophobic graphite. The dimensions of these sheets were consistent with those of β-sheets with extended peptide chains perpendicular to the long axis of the aggregate.

It had previously been shown[16,26] that Aβ cannot penetrate into zwitterionic lipid monolayers at high surface pressures. Adsorption at highly compressed anionic monolayers on water, however, can be explained in terms of weak electrostatic interactions between these phospholipids and Aβ. These interactions are possible because of low counterion concentrations in the subphase and, therefore, poor charge compensation of the anionic phospholipids combined with a low surface pH,[44] inducing a net positive charge in the peptide. Since the area occupied by a lipid molecule at high surface pressure remains in general the same during adsorption of the peptide (data not shown), one can conclude that the peptide is adsorbing at the monolayer but not penetrating into the chain region.

The electrostatic interactions with negatively charged lipids result in peptide adsorption. However, at modest salt concentrations the electrostatic interactions are screened and the peptide is removed from the surface. It may appear puzzling that the electrostatic repulsion between phospholipid head groups is increased on going from water to buffer—that is, closer to physiological conditions—but the attraction between head groups and Aβ is decreased. This can be explained by the fact that the Debye screening length decreases to 1 nm on going to 100 mM salt. Hence, since the head groups are closer than 1 nm, screening is not very effective and the increased charge density at the interface dominates. In contrast, the Aβ–head group distance is mostly above 1 nm, so the electrostatic interaction is mostly screened. When adsorbed on negatively charged monolayers the peptide should change the ionization state of the lipid molecules, acting as a buffer. As we know, the structure of a charged DPPG monolayer differs from that of a protonated one, so it may be expected that the structures of DPPG monolayers on water and on the peptide solution will differ as well. However, the DPPG structure is almost unchanged after Aβ adsorption. Probably there are two phenomena, compensating one another. On the one hand, the peptide changes the lipid ionization state, increasing the repulsion between lipid molecules. Increased repulsion results in a more tilted structure. On the other hand, interaction with lipid molecules may affect the head group orientation and hydration, which can change the tilt angle in the opposite direction.

Terzi et al.,[16] Bokvist et al.,[17] and Kakio et al.[19,20] have shown that the secondary structure of Aβ in the presence of negatively charged vesicles depends on the lipid-to-peptide ratio (L/P). A random coil→β-sheet→α-helix pathway has been observed in experiments with a constant peptide concentration and increasing lipid concentration. Accordingly, a random coil→α-helix→β-sheet pathway would be expected in monolayer experiments during the adsorption process (decreasing L/P ratio due to increasing peptide concentration at a fixed lipid concentration). However, no α-helical secondary structure was detected at the interface even at the beginning of the adsorption process, where the L/P ratio is large. Hence the question arises of what is the minimum peptide concentration detectable by IRRAS. In the case of another model peptide,[23] the first detectable IRRAS signal was observed at a peptide concentration of around 0.7 nm^2 per amino acid residue. At such a surface concentration, Aβ occupies an area of approximately 28 nm^2, corresponding to 65–70 DPPG molecules in the condensed state. At an L/P ratio of 65–70 one would expect α-helical secondary structure, as observed in the bulk state. However, the IRRAS signal of the peptide is at the resolution limit at such small surface concentrations, and much smaller than signals arising from the lipids and water, and so remains undetected. Additionally, the curvature of the system could also play a certain role, and the L/P ratio at planar monolayer surfaces maybe has to be larger than at curved vesicle surfaces to induce the transition to α-helix.

Comparison of LE and LC phases of anionic monolayers shows that the hydrophobic interactions between aliphatic chains in the condensed phases are much stronger than interactions between the lipid tails and the peptide. Insertion of the peptide into condensed monolayers is energetically unfavorable because it destabilizes the interchain interactions, so the peptide is squeezed out from a condensed monolayer at high surface pressures. A different situation is observed when

the lipid is in the LE phase: the tails are disordered and interchain interactions are weak. Obviously, the presence of the peptide does not disturb the monolayer packing to a larger extent. Aβ remains in such monolayers upon compression. At high surface pressures, however, the adsorbed peptide has to be additionally stabilized by weak electrostatic interactions.

Conclusion

Figure 10 summarizes the results of CD, GIXD, and IRRAS experiments. After pretreatment with HFIP, Aβ exhibits mainly random coil conformation in the bulk state. It adsorbs at the hydrophobic/hydrophilic air/water interface and penetrates into uncompressed lipid monolayers (Figure 10, top), and at the interface it adopts a β-sheet conformation, with the β-sheets oriented almost parallel to the surface. The current IRRAS and GIXD results demonstrate that the peptide has almost no influence on lipid phase behavior and structure. Compression of monolayers with inserted Aβ to surface pressures above 30 mN m^{-1} results in the squeezing out of the peptide. For zwitterionic phospholipids, both on water and buffer, the amide bands disappear; this indicates that the peptide even leaves the surface, independent of the lipid phase state. In the case of anionic phospholipids, the situation on comparison of monolayers on water or on buffer is different. On water, Aβ remains adsorbed at the negatively charged lipid monolayers independent of the phase state. Furthermore, only on water does Aβ adsorb at highly compressed anionic monolayers. Addition of salt forces the peptide to desorb from the condensed monolayer surface (Figure 10, bottom). On buffer, compression to 30 mN m^{-1} results in the disappearance of the peptide signal if the anionic monolayer is in a condensed state. In contrast, Aβ stays adsorbed at or partly penetrated into disordered anionic monolayers upon compression, but does not adsorb either at compressed ordered monolayers or at disordered monolayers in the presence of salt.

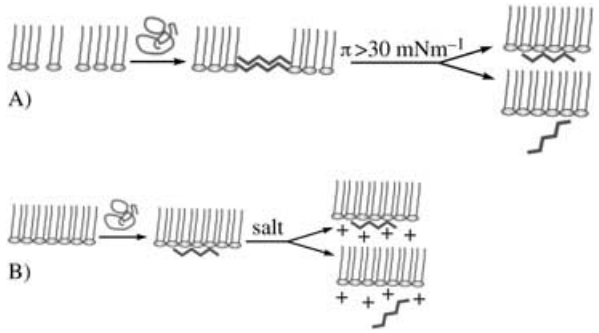

Figure 10. A) Schematic representation of Aβ insertion into uncompressed lipid monolayers at zero pressure (either liquid-expanded and gaseous phases or condensed and gaseous phases are coexisting). In the bulk state, the peptide is mainly in a random coil conformation. The inserted peptide adopts a β-sheet conformation at the interface. Compression of lipid monolayers with inserted Aβ to surface pressures above 30 mN m^{-1} results in the squeezing out of the peptide. The squeezed out peptide either leaves the interface (zwitterionic monolayers both on water and buffer or anionic condensed monolayers on buffer) or remains adsorbed (anionic monolayers on water, independent of the lipid phase state, or disordered fluid anionic monolayers on buffer). B) Aβ adsorption at negatively charged lipid monolayers at 30 mN m^{-1} on water. The adsorbed peptide adopts a β-sheet conformation at the interface. Upon addition of salt, the peptide either remains adsorbed (if the lipid monolayer is disordered) or it desorbs completely (if the monolayer is in a condensed state).

From these results, we conclude that Aβ readily adsorbs at hydrophobic surfaces and at charged hydrophilic surfaces in the absence of salt. An increasing surface peptide concentration results in conformational changes in the peptide's secondary structure. If a lateral pressure of 30 mN m^{-1} is assumed in bilayer membranes,[45,46] it is then very unlikely that the peptide would adsorb at membrane surfaces and influence their properties through interactions with phospholipids under physiological conditions. Either the membrane, as a dynamic system, has locally lower lateral pressure, so that the peptide can adsorb and penetrate into charged hydrophilic membrane surfaces, or other components of the membrane or complexing ions such as copper and zinc could be involved in the binding of Aβ to the membrane, resulting in its disruption or alteration.

Experimental Section

Materials: 1,2-Dipalmitoylphosphatidylcholine (DPPC), 1,2-dimyristoylphosphatidylcholine (DMPC), 1,2-dipalmitoylphosphatidylglycerol (DPPG), 1,2-dimyristoylphosphatidylglycerol (DMPG), and 1,2-dipalmitoylphosphatidylserine (DPPS) were purchased from Sigma with purities of 99% and were used as received. They were spread onto the air/water interface from a 1 mM methanol (Sigma)/chloroform (Baker) (1:3, *v/v*) solution. The Amyloid β (1–40) peptide was obtained from Bachem (Switzerland). The peptide was first dissolved in hexafluoroisopropanol (HFIP) to destroy possible aggregates[47] and stored in a refrigerator. Before measurements, HFIP was evaporated under a nitrogen stream and the peptide was dissolved in water or buffer at pH 7.5 (10 mM potassium phosphate, 100 mM NaCl). The secondary structure of the peptide was checked by circular dichroism (CD) spectroscopy (Jasco J-715, Japan). The peptide was found to have predominantly random coil conformation after such a pretreatment. All solutions were prepared with Milli-Q deionized water (resistivity of 18.2 MΩ cm).

Methods: All measurements were carried out in PTFE Langmuir troughs. The surface pressure was monitored through a Wilhelmy microbalance with use of a filter paper plate. Two different setups were used to adsorb the peptide at the lipid monolayer or the air/water (buffer) interface. Either the lipid was spread onto the freshly cleaned surface of a subphase containing Aβ (0.185 μM or 0.3 μM) or the peptide was injected into the subphase beneath the phospholipid monolayer, which was compressed to 30 mN m^{-1}.

Synchrotron grazing incidence X-ray diffraction (GIXD) measurements were carried out at 20 °C by use of the liquid-surface diffractometer on the undulator beamline BW1 of HASYLAB, DESY (Hamburg, Germany).[48–50] The intensity of the diffracted beam was detected with a linear position-sensitive detector (OEM-100-M, Braun, Garching, Germany) as a function of the vertical scattering angle α_f. The in-plane (horizontal) scattering angle 2Θ was varied by rotation of the detector and Soller collimator. The accumulated position-resolved counts were corrected for polarization, effective area, and Lorentz factor. Model peaks, taken as Lorentzian in the in-plane direction and as Gaussian in the out-of-plane direction, were least-squares fitted to the measured intensities.

IRRA spectra were recorded on an IFS 66 FTIR spectrometer (Bruker, Germany) fitted with a liquid nitrogen-cooled mercury cadmium telluride detector and the XA 511 external reflection accessory. The IR beam was conducted out of the spectrometer and focused onto the water surface of the Langmuir trough. The angle of incidence was varied between 32° and 62° with respect to the surface normal and the IR beam was polarized by use of a polarizer in the plane of incidence (*p*) or perpendicular to this plane (*s*). Measurements were performed by use of a trough containing two compartments and a trough shuttle system. One compartment contained the monolayer system under investigation (sample), whereas the other (reference) was filled with pure water (buffer). The single-beam reflectance spectrum from the reference trough was used as background to the single-beam reflectance spectrum of the monolayer in the sample trough to calculate the reflection absorption spectrum as $-\log(R/R_0)$ in order to eliminate the water vapor signal. To maintain a constant water vapor content the setup was placed in a hermetically sealed container. FTIR spectra were collected at 8 cm^{-1} resolution with use of 200 scans for *s*-polarized light and 400–800 scans for *p*-polarized light.

There are several theoretical approaches describing the dependence of IRRAS band intensities on the incident angle and transition dipole moment orientation. In the current work we used the mathematical model of Kuzmin et al.[51,52] and the formalism published by Mendelsohn et al.[34] for monolayers at the air/water interface.

Acknowledgements

This work was supported by the Deutsche Forschungsgemeinschaft (BR 1378/8-2). We gratefully acknowledge beamtime at HASYLAB, DESY (Hamburg, Germany) and Dr. K. Kjaer's help with the beamline set-up.

Keywords: amyloid peptides · IR spectroscopy · monolayers · phospholipids · secondary structure · X-ray diffraction

[1] J. Kang, H. G. Lemaire, A. Unterbeck, J. M. Salbaum, C. L. Masters, K. H. Grzeschik, G. Multhaup, K. Beyreuther, B. Mullerhill, *Nature* **1987**, *325*, 733 – 736.
[2] C. Haass, D. J. Selkoe, *Nature* **1998**, *391*, 339 – 340.
[3] D. M. Walsh, D. M. Hartley, Y. Kusumoto, Y. Fezoui, M. M. Condron, A. Lomakin, G. B. Benedek, D. J. Selkoe, D. B. Teplow, *J. Biol. Chem.* **1999**, *274*, 25 945 – 25 952.
[4] D. M. Walsh, A. Lomakin, G. B. Benedek, M. M. Condron, D. B. Teplow, *J. Biol. Chem.* **1997**, *272*, 22 364 – 22 372.
[5] D. B. Teplow, *Amyloid* **1998**, *5*, 121 – 142.
[6] C. Soto, B. Frangione, *Neurosci. Lett.* **1995**, *186*, 115 – 118.
[7] G. Forloni, *Curr. Opin. Neurol.* **1996**, *9*, 492 – 500.
[8] D. J. Selkoe, *Science* **1997**, *275*, 630 – 631.
[9] R. P. Mason, R. F. Jacob, M. F. Walter, P. E. Mason, N. A. Avdulov, S. V. Chochina, U. Igbavboa, W. G. Wood, *J. Biol. Chem.* **1999**, *274*, 18 801 – 18 807.
[10] C. M. Yip, E. A. Elton, A. A. Darabie, M. R. Morrison, J. McLaurin, *J. Mol. Biol.* **2001**, *311*, 723 – 734.
[11] C. M. Yip, J. McLaurin, *Biophys. J.* **2001**, *80*, 1359 – 1371.
[12] S. A. Waschuk, E. A. Elton, A. A. Darabie, P. E. Fraser, J. McLaurin, *J. Biol. Chem.* **2001**, *276*, 33 561 – 33 568.
[13] D. G. Lynn, S. C. Meredith, *J. Struct. Biol.* **2000**, *130*, 153 – 173.
[14] R. Bhatia, H. Lin, R. Lal, *FASEB J.* **2000**, *14*, 1233 – 1243.
[15] C. Behl, *Cell Tissue Res.* **1997**, *290*, 471 – 480.
[16] E. Terzi, G. Holzemann, J. Seelig, *Biochemistry* **1997**, *36*, 14 845 – 14 852.
[17] M. Bokvist, F. Lindström, A. Watts, G. Gröbner, *J. Mol. Biol.* **2004**, *335*, 1039 – 1049.
[18] C. C. Curtain, F. E. Ali, D. G. Smith, A. I. Bush, C. L. Masters, K. J. Barnham, *J. Biol. Chem.* **2003**, *278*, 2977 – 2982.
[19] A. Kakio, S. Nishimoto, K. Yanagisawa, Y. Kozutsumi, K. Matsuzaki, *J. Biol. Chem.* **2001**, *276*, 24 985 – 24 990.
[20] A. Kakio, S. Nishimoto, K. Yanagisawa, Y. Kozutsumi, K. Matsuzaki, *Biochemistry* **2002**, *41*, 7385 – 7390.
[21] G. Brezesinski, H. Möhwald, *Adv. Colloid Interface Sci.* **2003**, *100*, 563 – 584.
[22] K. Kjaer, J. Als-Nielsen, C. A. Helm, L. A. Laxhuber, H. Möhwald, *Phys. Rev. Lett.* **1987**, *58*, 2224 – 2227.
[23] A. Kerth, A. Erbe, M. Dathe, A. Blume, *Biophys. J.* **2004**, *86*, 3750 – 3758.
[24] Z. Xu, J. W. Brauner, C. R. Flach, R. Mendelsohn, *Langmuir* **2004**, *20*, 3730 – 3733.
[25] D. Dieudonne, R. Mendelsohn, R. S. Farid, C. R. Flach, *Biochim. Biophys. Acta* **2001**, *1511*, 99 – 112.
[26] E. Maltseva, G. Brezesinski, *ChemPhysChem* **2004**, *5*, 1185 – 1190.
[27] C. Ege, K. Y. C. Lee, *Biophys. J.* **2004**, *87*, 1732 – 1740.
[28] N. N. Kalnin, I. A. Baikalov, S. Y. Venyaminov, *Biopolymers* **1990**, *30*, 1273 – 1280.
[29] S. Y. Venyaminov, N. N. Kalnin, *Biopolymers* **1990**, *30*, 1243 – 1257.
[30] Y. N. Chirgadze, N. A. Nevskaya, *Biopolymers* **1976**, *15*, 607 – 625.
[31] H. Hussain, A. Kerth, A. Blume, J. Kressler, *J. Phys. Chem. B* **2004**, *108*, 9962 – 9969.
[32] A. Meister, A. Kerth, A. Blume, *J. Phys. Chem. B* **2004**, *108*, 8371 – 8378.
[33] T. Buffeteau, E. Le Calvez, S. Castano, B. Desbat, D. Blaudez, J. Dufourcq, *J. Phys. Chem. B* **2000**, *104*, 4537 – 4544.
[34] R. Mendelsohn, J. W. Brauner, A. Gericke, *Annu. Rev. Phys. Chem.* **1995**, *46*, 305 – 334.
[35] R. A. Macphail, H. L. Strauss, R. G. Snyder, C. A. Elliger, *J. Phys. Chem.* **1984**, *88*, 334 – 341.
[36] R. G. Snyder, H. L. Strauss, C. A. Elliger, *J. Phys. Chem.* **1982**, *86*, 5145 – 5150.
[37] M. M. Sacre, E. M. Elmashak, J. F. Tocanne, *Chem. Phys. Lipids* **1977**, *20*, 305 – 318.
[38] M. M. Sacre, J. F. Tocanne, *Chem. Phys. Lipids* **1977**, *18*, 334 – 354.
[39] F. Lakhdarghazal, J. L. Tichadou, J. F. Tocanne, *Eur. J. Biochem.* **1983**, *134*, 531 – 537.
[40] A. Dicko, H. Bourque, M. Pezolet, *Chem. Phys. Lipids* **1998**, *96*, 125 – 139.
[41] A. Aroti, E. Leontidis, E. Maltseva, G. Brezesinski, *J. Phys. Chem. B* **2004**, *108*, 15 238 – 15 245.
[42] C. Ege, J. Majewski, G. Wu, K. Kjaer, K. Y. C. Lee, *ChemPhysChem* **2005**, *6*, 226 – 229.
[43] T. Kowalewski, D. M. Holtzman, *Proc. Natl. Acad. Sci. USA* **1999**, *96*, 3688 – 3693.
[44] E. Le Calvez, D. Blaudez, T. Buffeteau, B. Desbat, *Langmuir* **2001**, *17*, 670 – 674.
[45] A. Seelig, *Biochim. Biophys. Acta* **1987**, *899*, 196 – 204.
[46] A. Blume, *Biochim. Biophys. Acta* **1979**, *557*, 32 – 44.
[47] W. B. Stine, K. N. Dahlgren, G. A. Krafft, M. J. LaDu, *J. Biol. Chem.* **2003**, *278*, 11 612 – 11 622.
[48] R. Rietz, W. Rettig, G. Brezesinski, W. G. Bouwman, K. Kjaer, H. Möhwald, *Thin Solid Films* **1996**, *285*, 211 – 215.
[49] D. Jacquemain, F. Leveiller, S. P. Weinbach, M. Lahav, L. Leiserowitz, K. Kjaer, J. Als-Nielsen, *J. Am. Chem. Soc.* **1991**, *113*, 7684 – 7691.
[50] J. Als-Nielsen, D. Jacquemain, K. Kjaer, F. Leveiller, M. Lahav, L. Leiserowitz, *Phys. Rep.* **1994**, *246*, 252 – 313.
[51] V. L. Kuzmin, V. P. Romanov, L. V. Kuzmin, *Opt. Spektrosk.* **1992**, *72*, 227 – 238.
[52] V. L. Kuzmin, A. V. Mikhailov, *Opt. Spektrosk.* **1981**, *51*, 691 – 695.

Received: April 23, 2005

